Skin cancer & cell discrimination using mid-IR spectroscopy

Results from MINERVA WP8

WP8 Partners: WWU, EXETER, GHNT, UPVLC

MId- to NEaR infrared spectroscopy
for improVed medical diAgnostics
MINERVA

Westfälische Wilhelms-Universität Münster

Introduction and Motivation

Develop mid-IR spectroscopy for skin cancer diagnostics:

- Definition of stable cell and tissue standards for continuous and reproducible testing conditions

Development and testing of in vitro skin models with increasing complexicity:

- Single cell lines
- Mixed fluorescence labelled cell lines
- 3D Human Skin Equivalents
- 3D height adjustable Melanoma models

Skin cell types

Tumor and non-tumor cell lines used for mid-IR spectroscopy. Cell lines representing the major cellular skin constituents keratinocytes and fibroblasts (NIH-3T3, HaCaT). Skin cancer cell types (A-375 and SK-MEL-28 cells)

Cell line	Species	Origin	Provider	Catalogue number
A-375	*H. sapiens*	Skin, malignant melanoma	CLS	300110
HaCaT	*H. sapiens*	Skin, kerationcytes	CLS	-
NIH-3T3	*M. musculus*	Embryo, fibroblasts	DSMZ	ACC 59
SK-MEL-28	*H. sapiens*	Skin, malignant melanoma	CLS	300337

Standardization of dried samples for substrates, fixation, stability and reproducibility

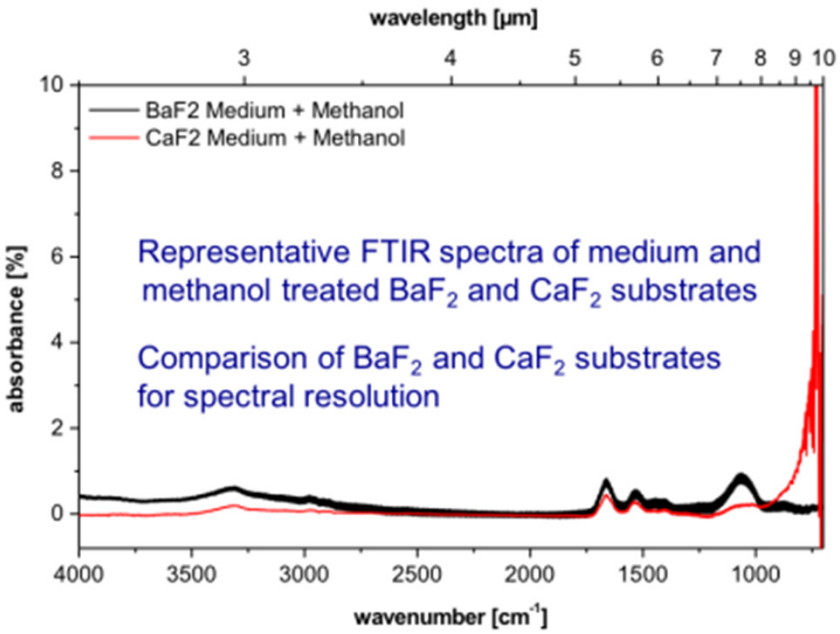

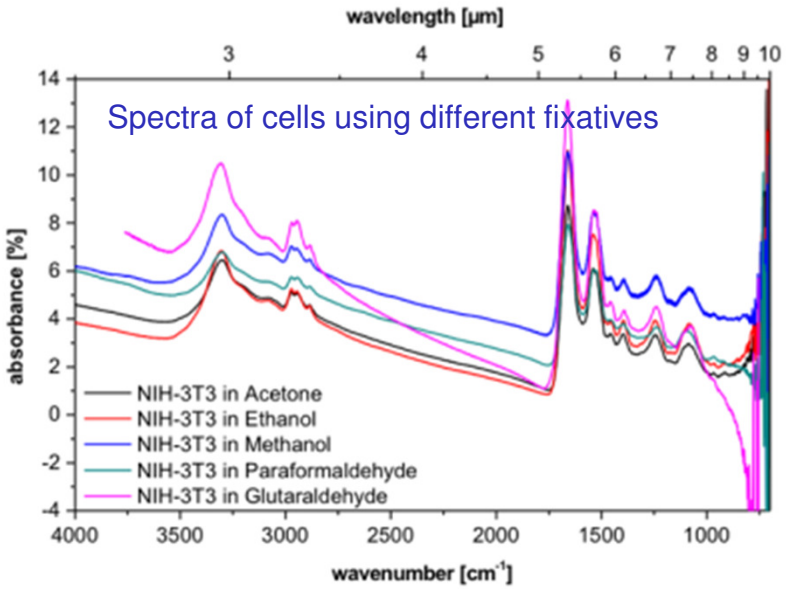

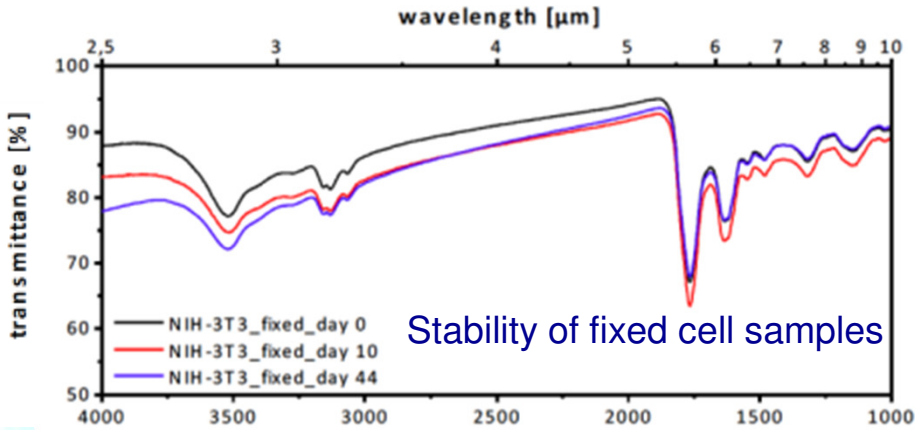

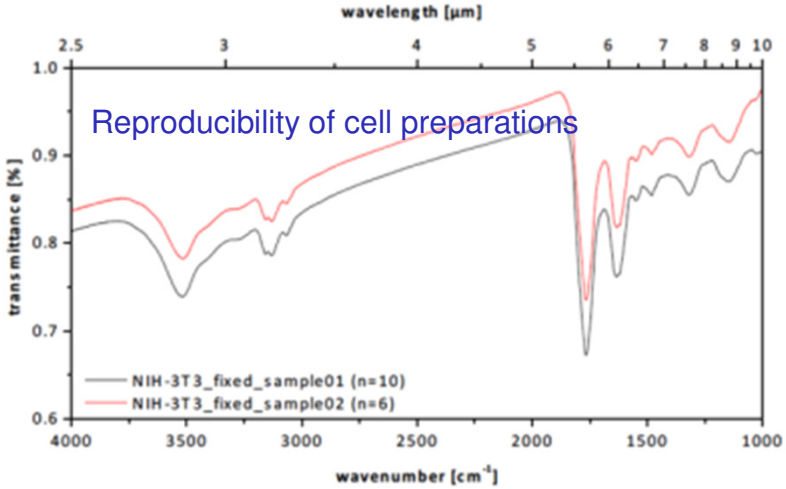

Spectral imaging of cancer and non-cancer cells on the same substrate

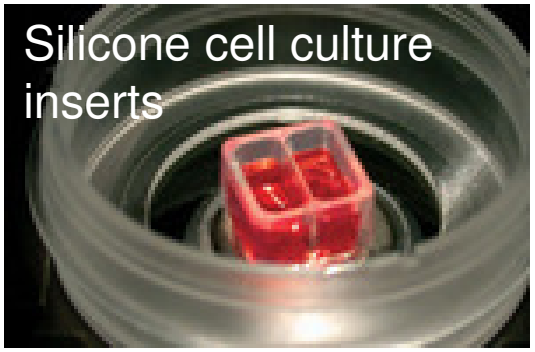

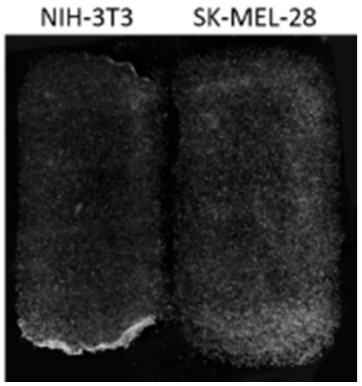

Representative phase contrast image of NIH-3T3 and SK-MEL-28 on a CaF_2 substrate.

SK-MEL-28 **NIH-3T3**

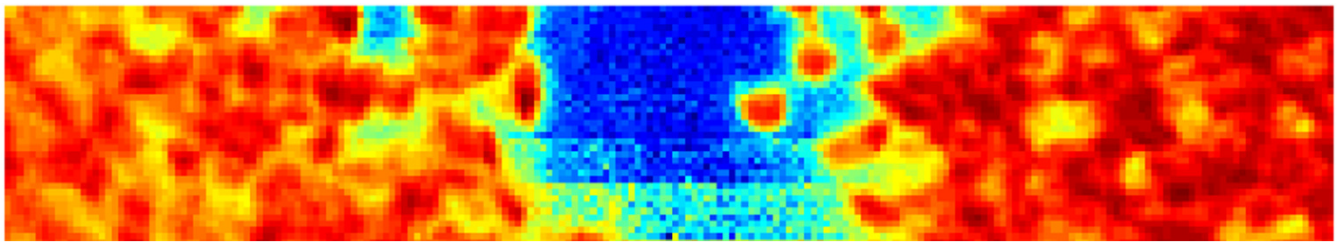

Intensity of the Amide I peak at 1650 cm^{-1}

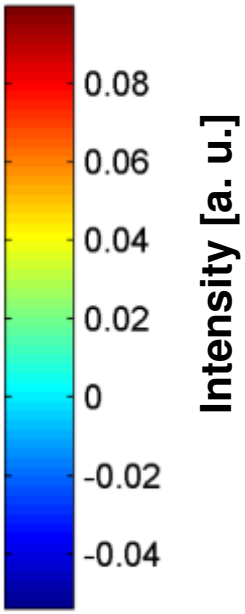

Comparison of skin cancer related cell lines

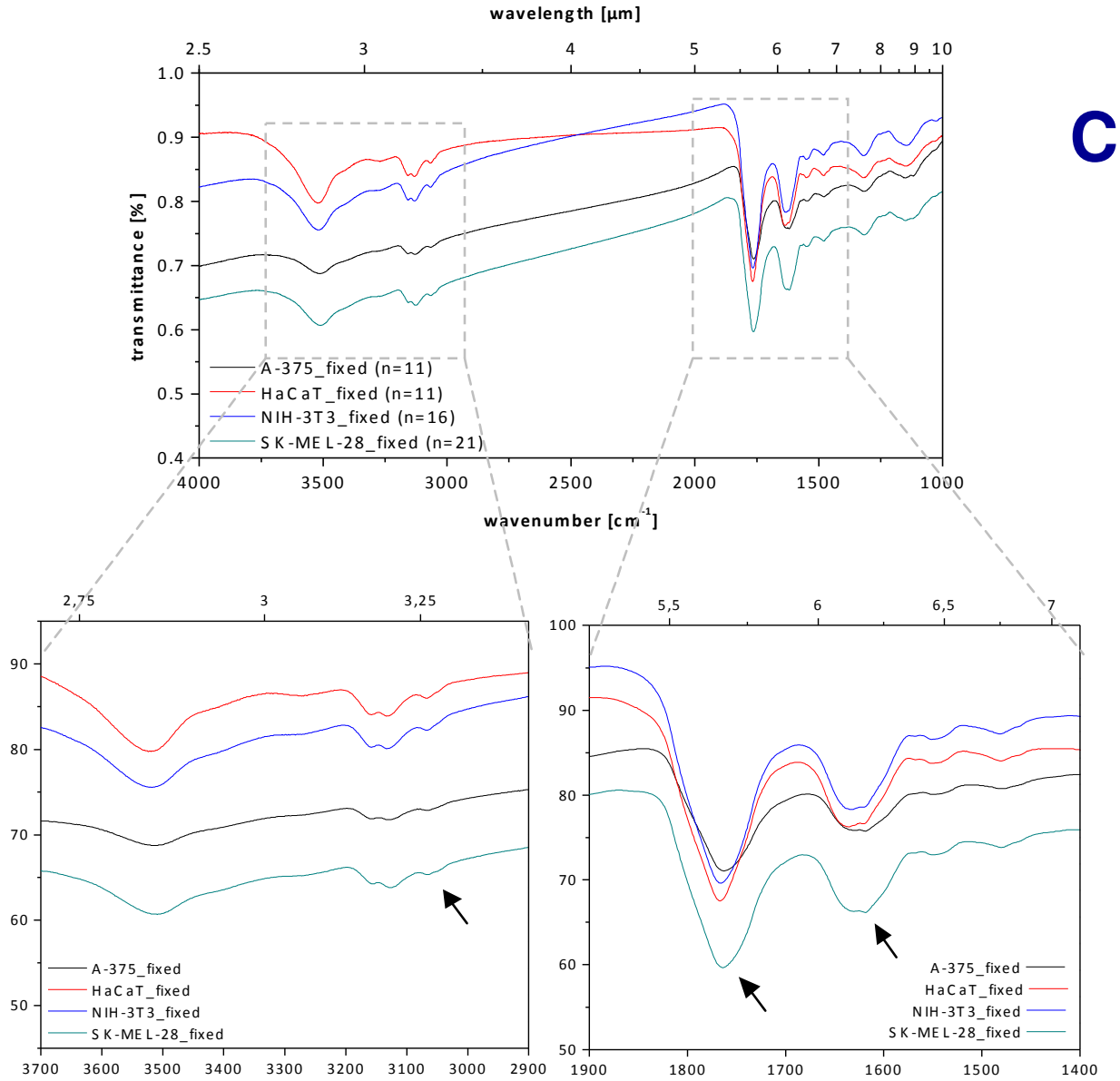

Comparison of the averaged MID-IR-spectra of the tumor cell lines A-375 and SK-MEL-28 and the non-tumor cell lines HaCaT and NIH-3T3.

Arrows in the magnified areas indicate spectral shifts and differences.

Mid-IR differentiation of skin cell types – first generation MINERVA algorithms

Results from a preliminary PCA in the fingerprint region (850 cm-1 to 1800 cm-1) performed in GHNT

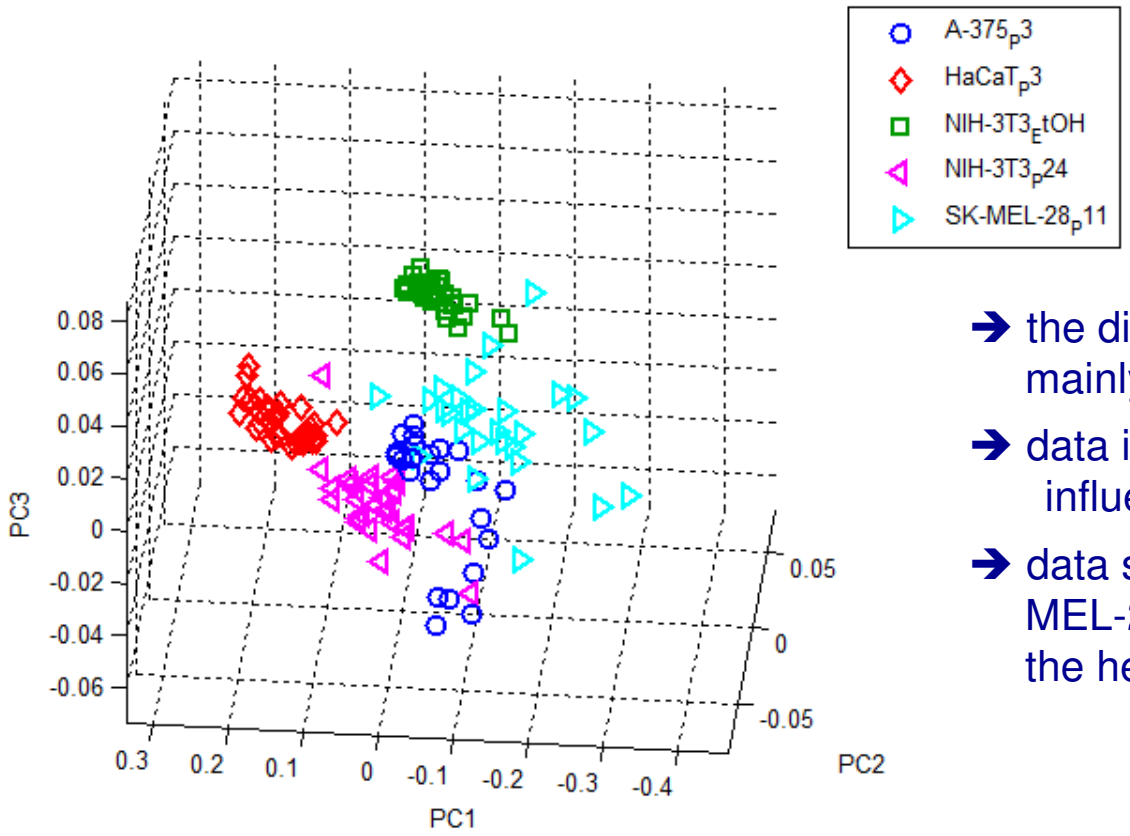

- ➔ the different cell lines appear mainly separated
- ➔ data indicates a spectral influence of the ethanol fixation
- ➔ data scattering of A-375 and SK-MEL-28 reflects the heterogeneity of cancer cells

Mixed fluorescence labeled skin cancer cell types on a single $CaFl_2$ substrate

Example: NIH-3T3, HaCaT, SK-Mel-28

Fluorescence (merged)

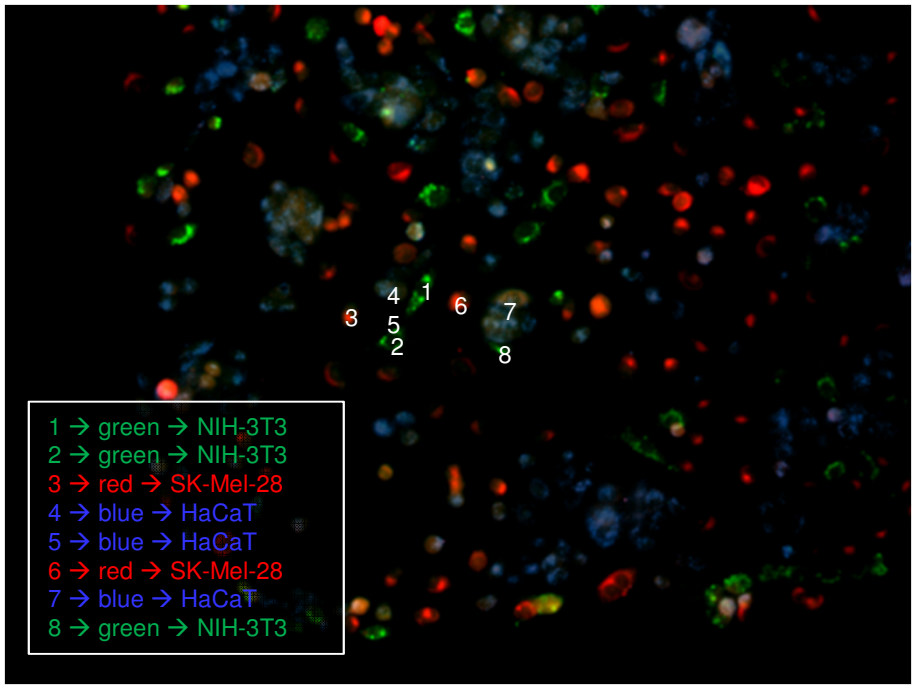

Fluorescence + bright field (merged)

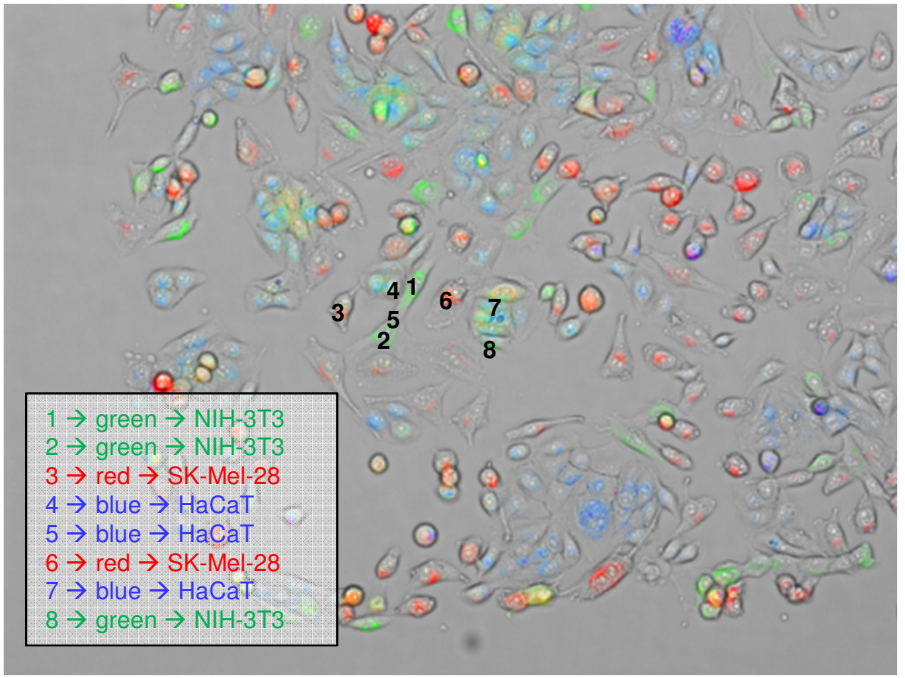

Green → Vybrant™ DiO Cell-Labeling Solution
Blue → Ibidi Fuse-It^{IR}
Red → Vybrant™ DiD Cell-Labeling Solution

mid-IR spectra of mixed fluorescence labeled cell types on a $CaFl_2$ substrate

MINERVA
improved medical diagnostics

Example: NIH-3T3, HaCaT, SK-Mel-28

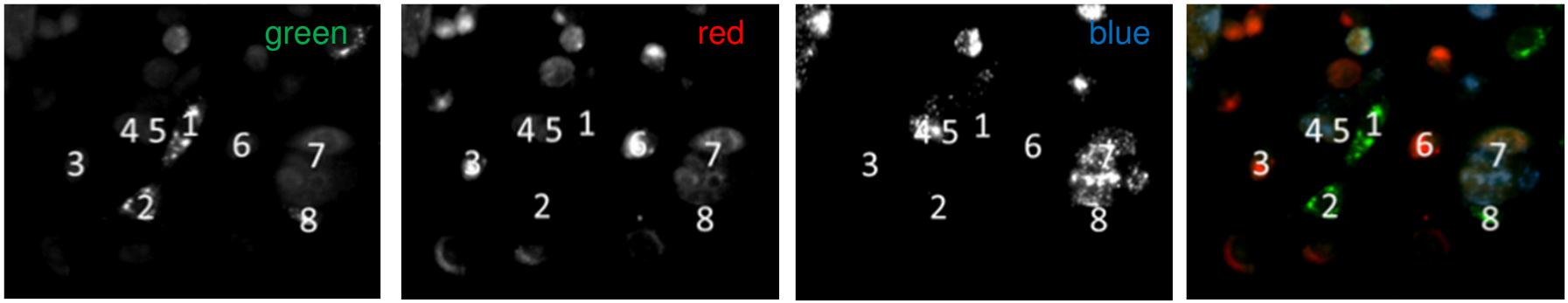

Example: Acquired midIR spectra of selected single cells

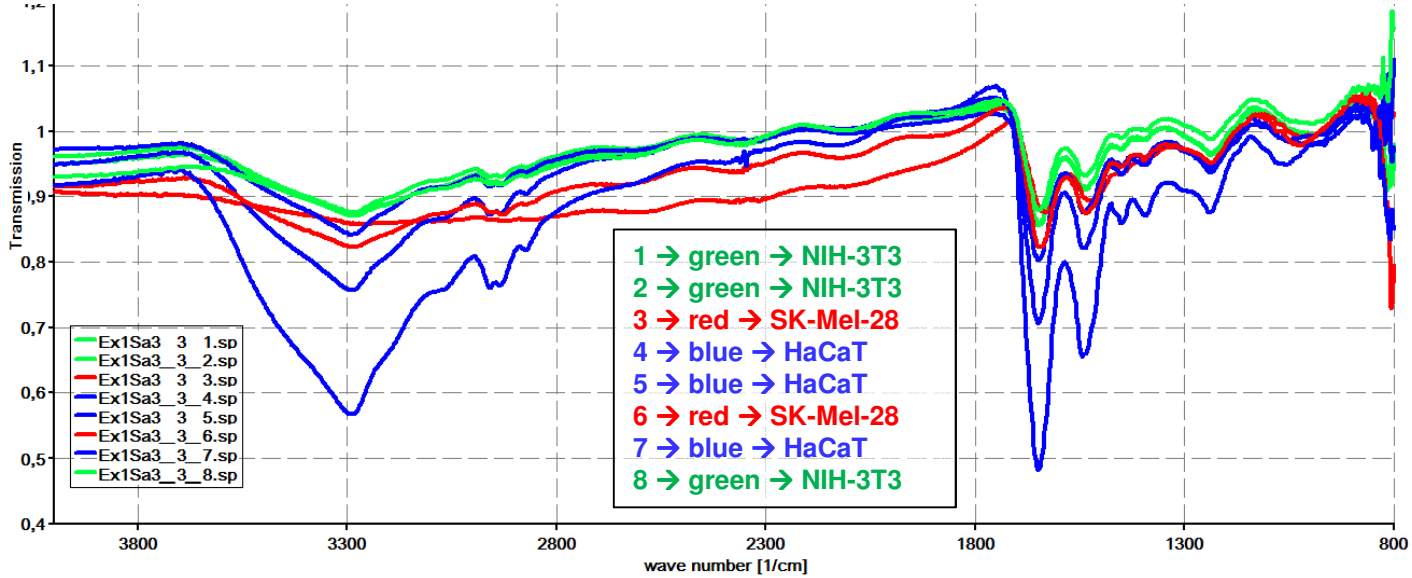

Westfälische Wilhelms-Universität Münster

Determination of mean cell thickness and area covered by single cells with digital holographic microscopy (DHM)

Representative images of single cells

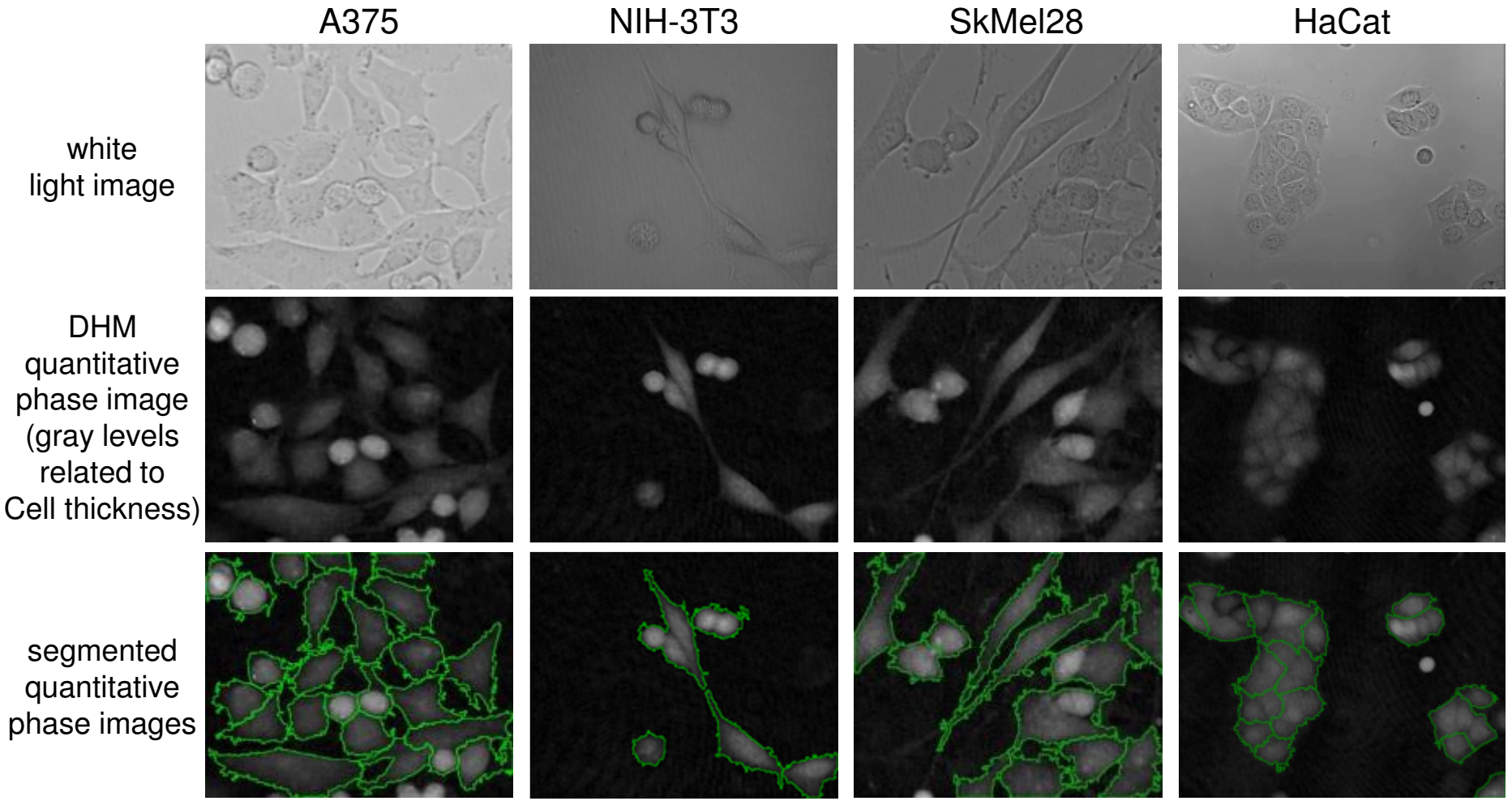

Determination of mean cell thickness and area covered by single cells with digital holographic microscopy (DHM)

Mean cell thickness

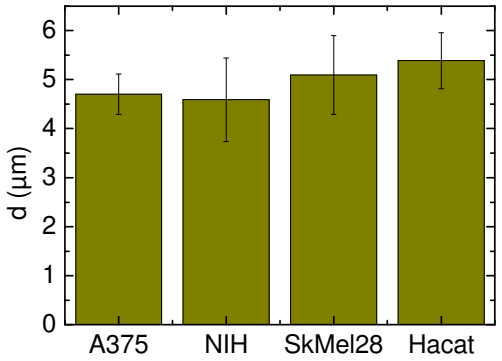

Mean surface area covered by a single cell

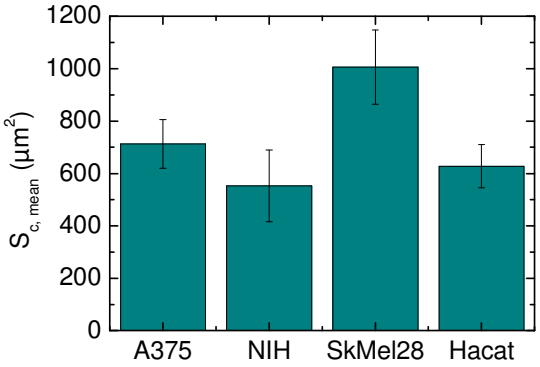

Cell type	N (# cells)	d (µm)	$S_{c, mean}$ (µm^2)
A375	90	4.7±0.4	712±93
NIH-3T3	85	4.6±0.9	553±137
SkMel28	95	5.1±0.8	1006±142
HaCat	123	5.4±0.6	627±83

Reference samples (pure dyes+BSA on CaF_2) for mid-IR measurements and algorithm training

- **BSA:**
  Bovine Serum Albumin 15% in PBS
- **VybrantDiO (red)/DiD (gree), FuseIt IR (ruby)**:
  Fluorescence Dyes
- **Medium:**
  supplemented cell culture media

➔ Correlative data for mid-IR analysis

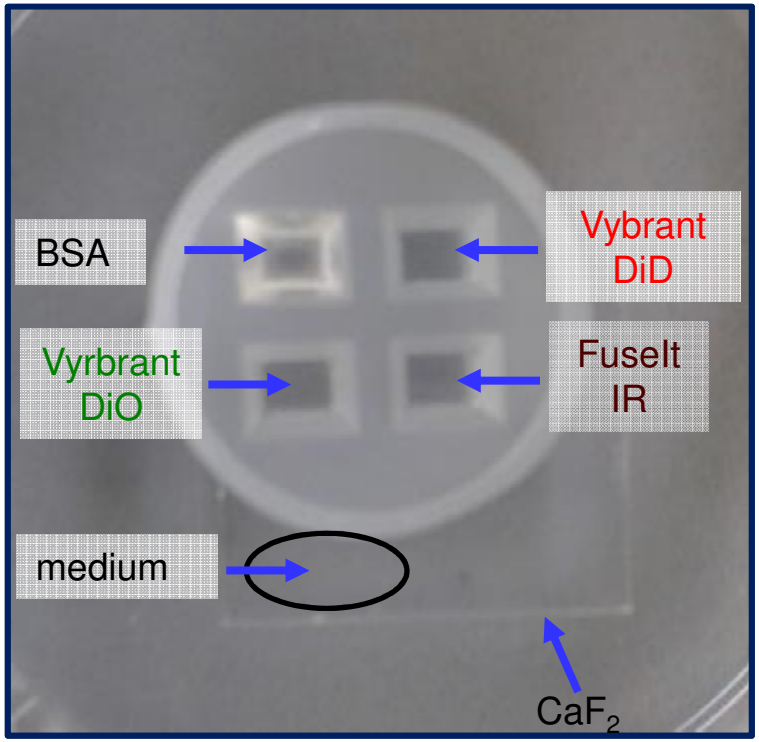

Mid-IR differentiation of skin cell types – improved and trained MINERVA algorithms

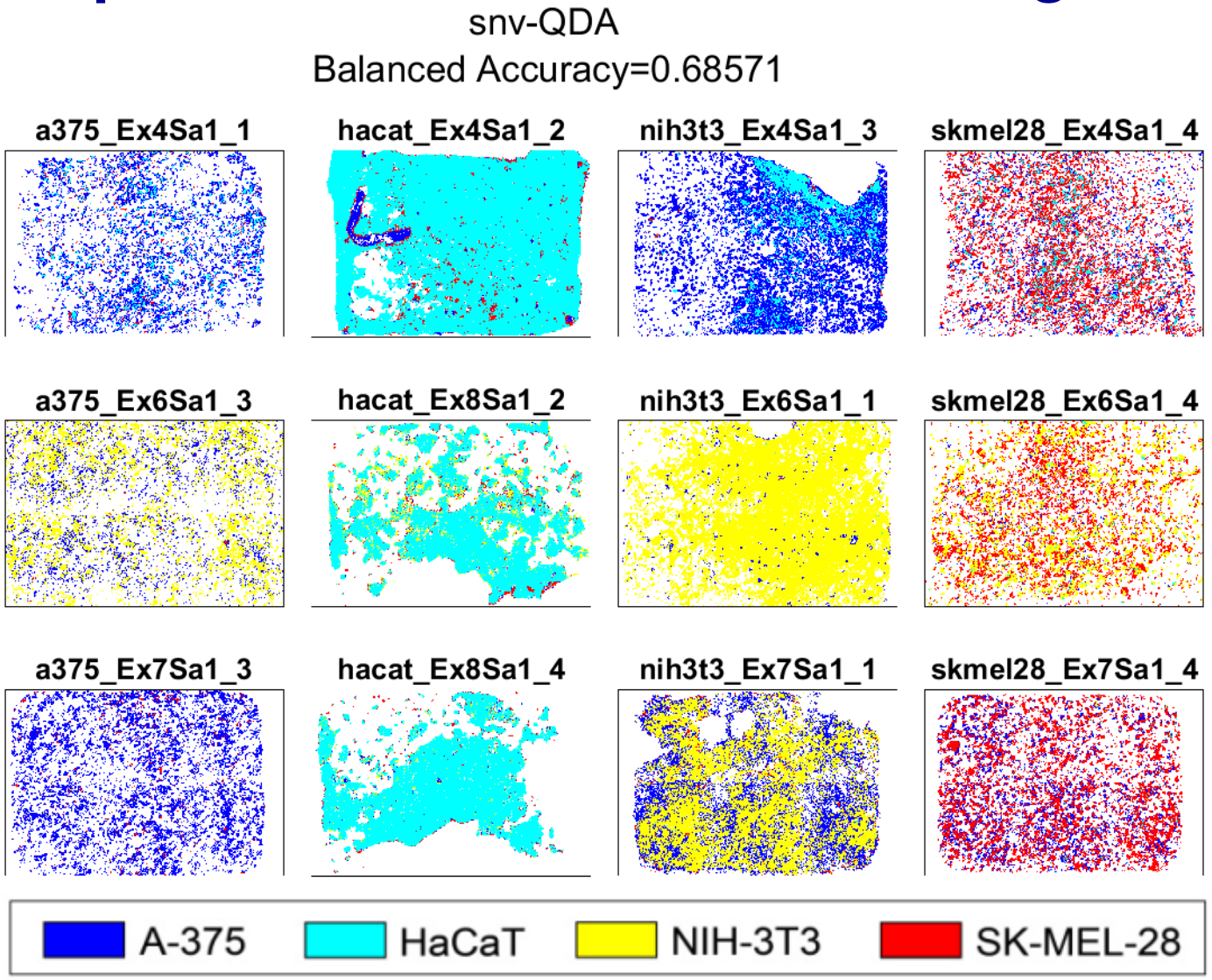

Pseudocolor images displaying the predicted labels assigned during the classification, as shown in the legend.. To assign the labels, the images from each row were left out as the test set and the algorithms were trained with the rest of images. Spectra were pre-processed with the Standard Normal Variate (SNV) transform. The classification algorithm was Quadratic Discriminant Analysis (QDA). **The Balanced (or Weighted) Accuracy of the overall dataset was 68.6%.**

Fully differentiated 3D skin equivalents for mid-IR imaging

Fixation with 10 % Formalin (without, carrier membrane)

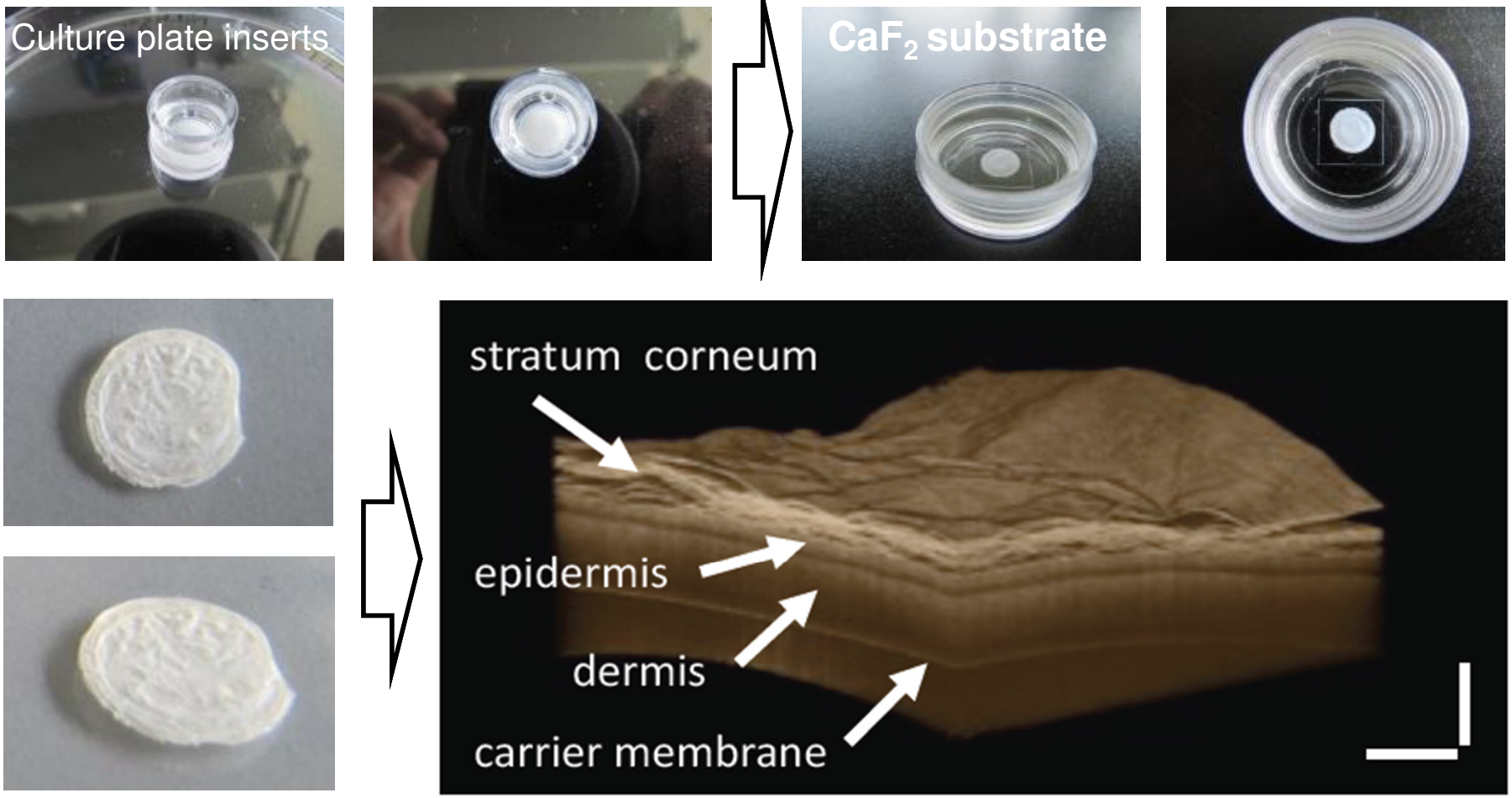

Left: Dried 3D samples for reflective and transmission spectroscopy; right representative optical coherence tomography image of the established 3D tissue models. Scale bars are equal to 250 µm.

Establishment of 3D skin equivalents for midIR imaging

Analysis of tissue density, with digital holographic microcopy

bright field

quantitative DHM phase contrast

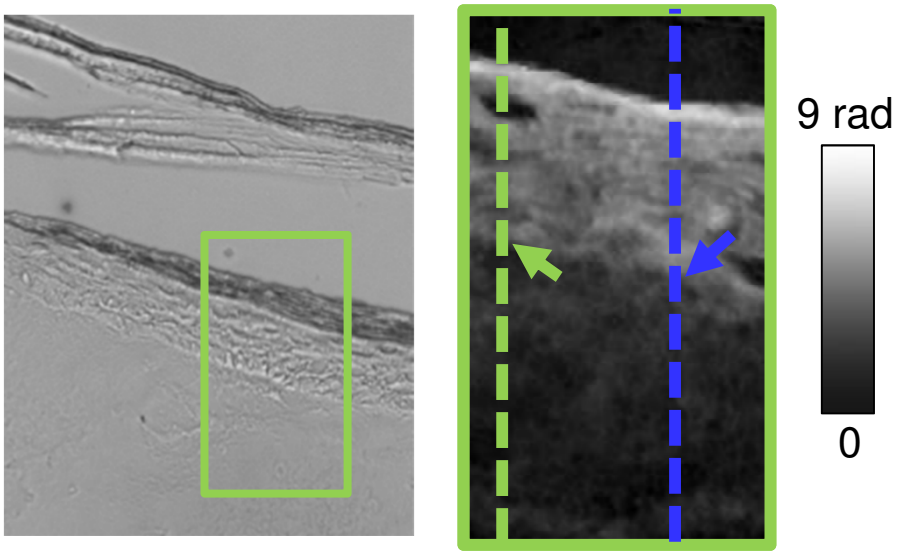

thickness: 7µm, 20x, Ethanol

tissue refractive index ➔ tissue density

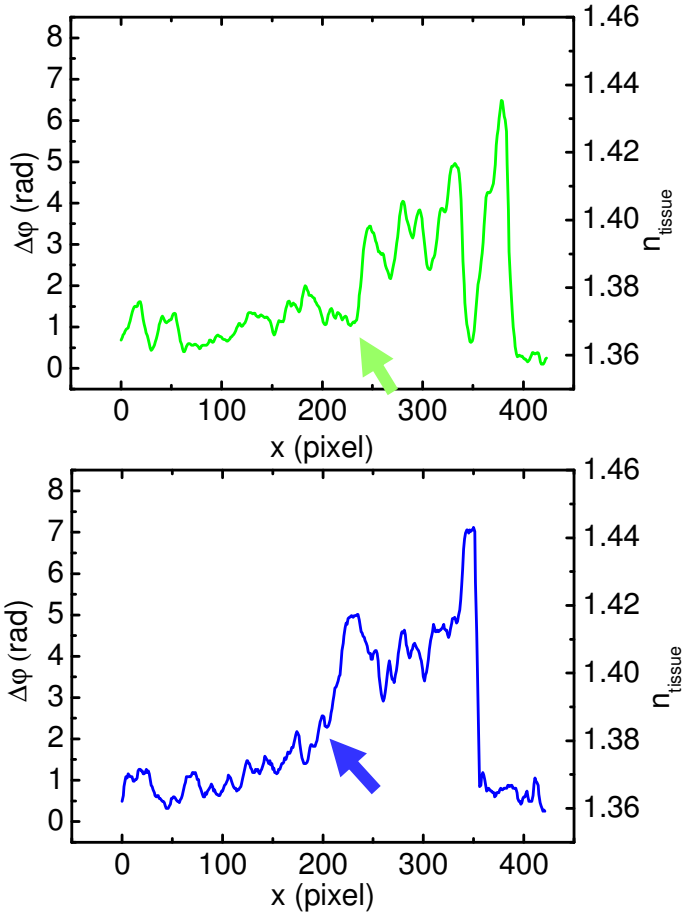

➔ Similar optical properties like cryostat sections

Method: P. Lenz, et al., Int. Biol. 5, 624-630 (2013)

Spectral data from on dissected human skin equivalents

Example: 16µm slice

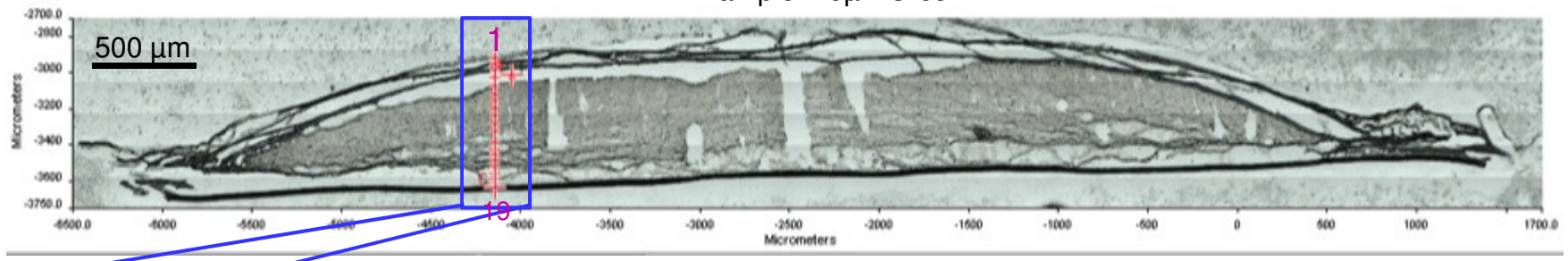

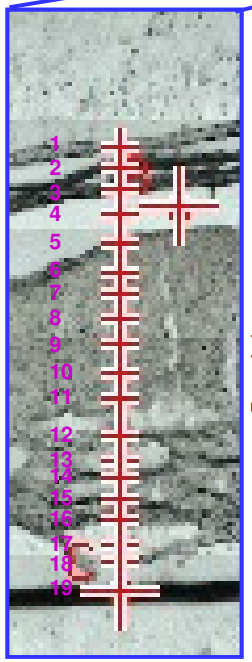

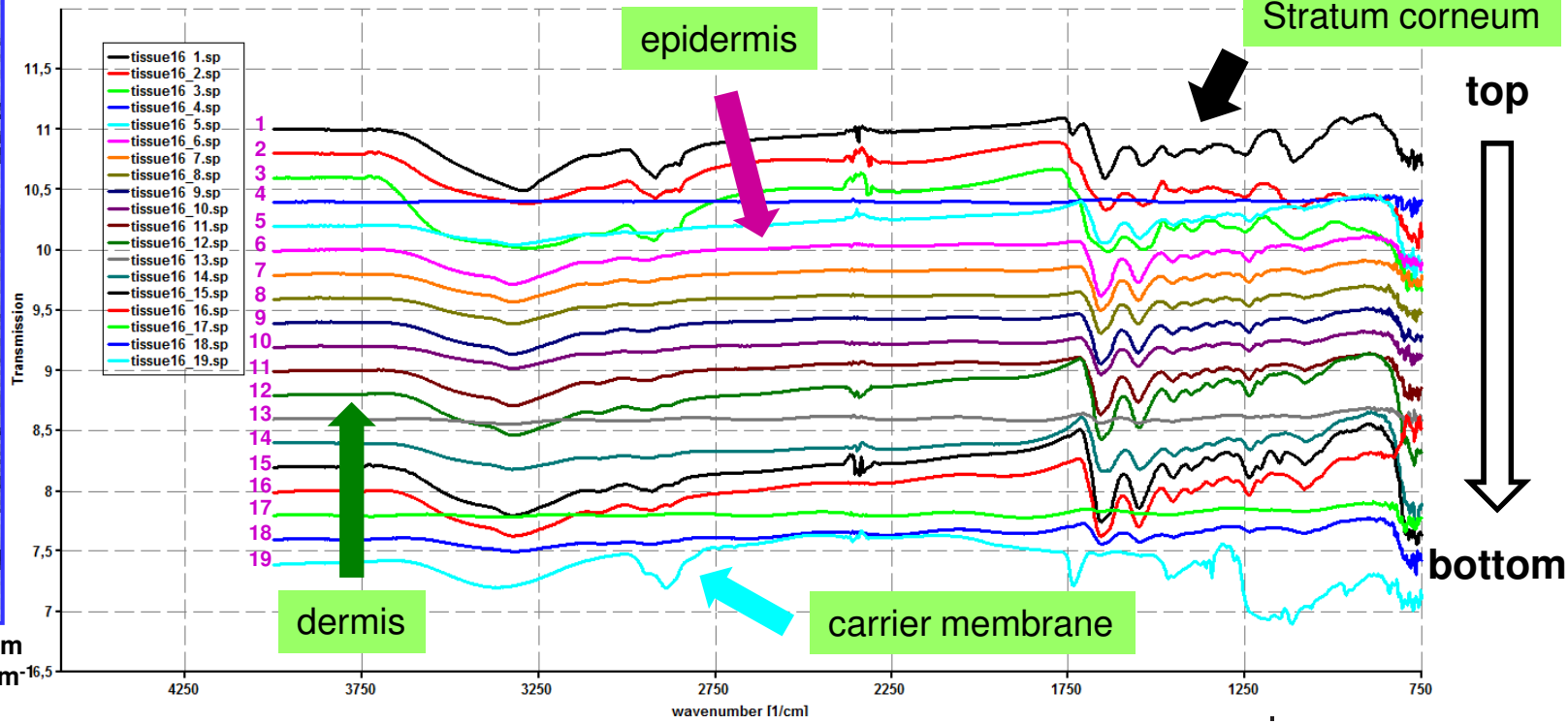

Aperture: 30 x 30 µm
Spectral width: 4 cm^{-1}
16 Scans

Spectral data from on dissected human skin equivalents

Comparison of averaged spectra

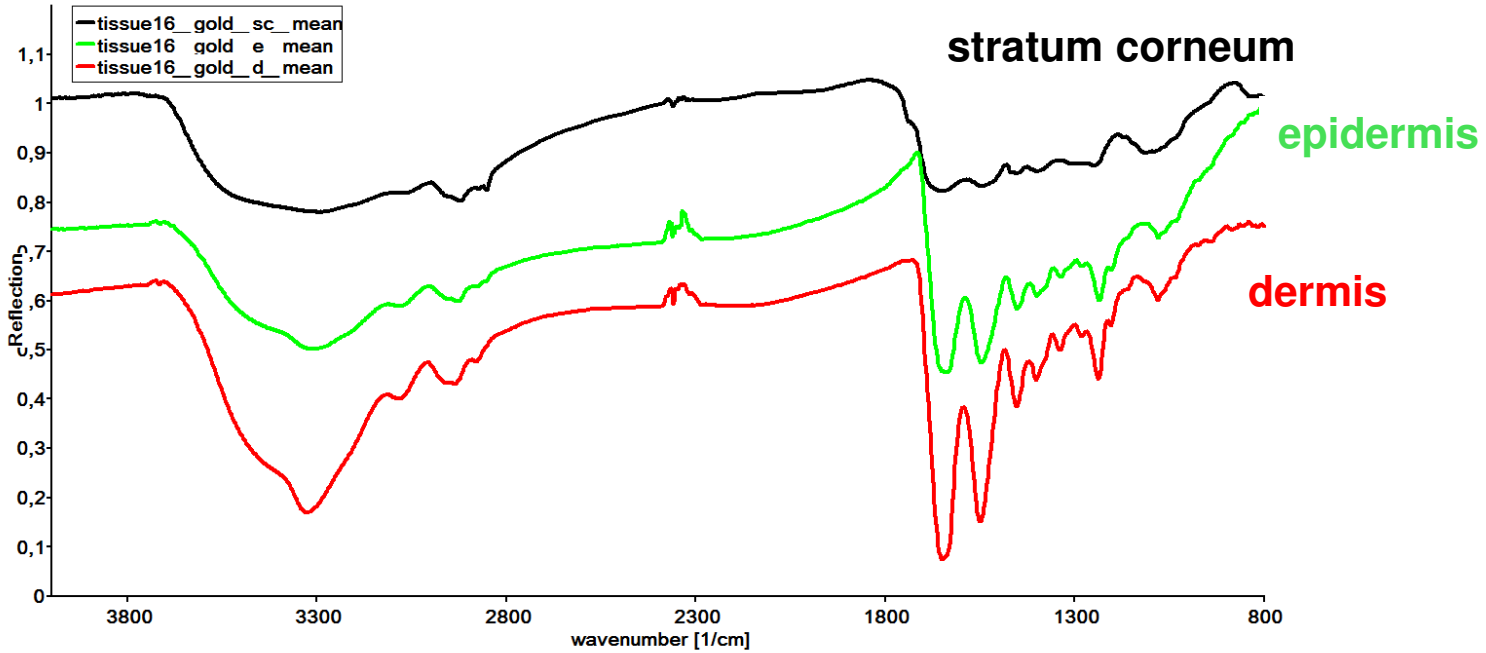

➔ **Clear differences between stratum corneum and epidermis / dermis**

mid-IR spectral analysis of 3D skin equivalents

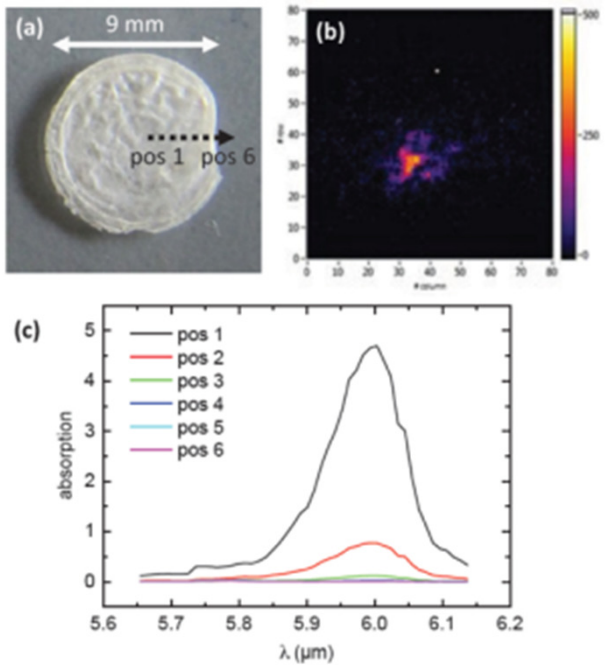

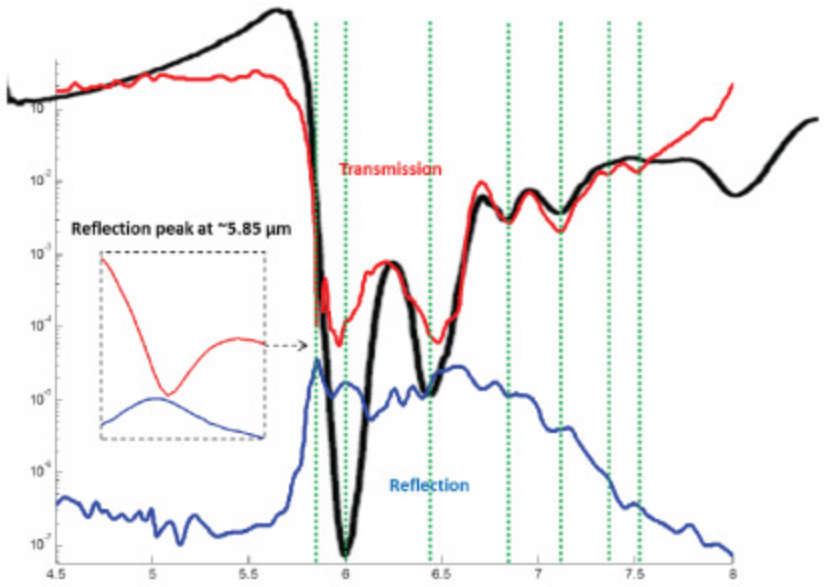

(data collected at DTU in transmission)

➔ Supercontinuum radiation penetrates more than 500 μm into 3D skin equivalents

➔ also gives insights into the scattering properties of tissue in mid-IR range.

➔ Further investigations are required to interpreted the observed effects

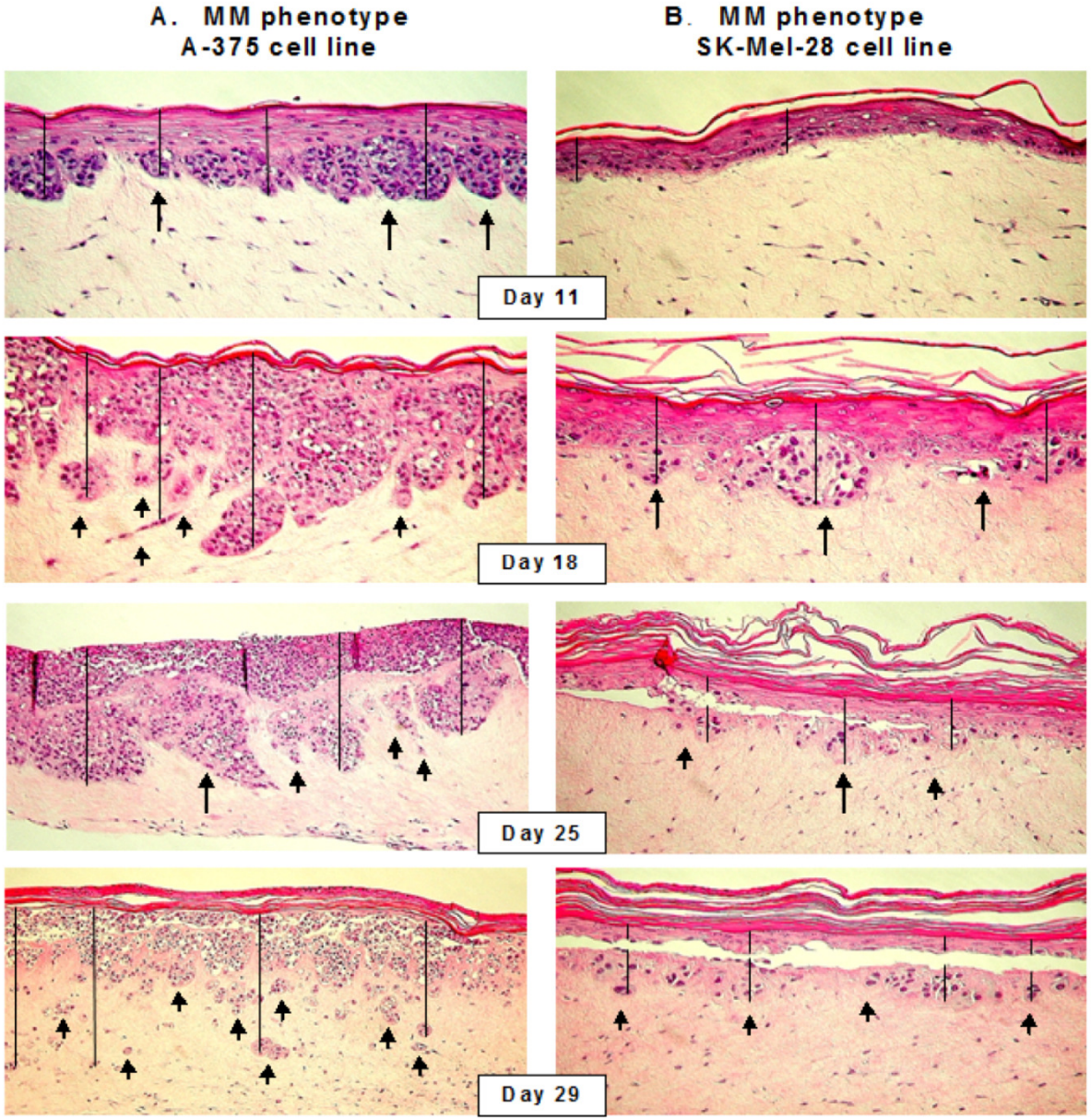

3D melanoma model

H&E stained sections of 3D skin equivalens with included skin tumors (from Klausner et al. Journal of investigative Dermatology 131, 10013-1917 (2011). The distribution of the tumors is inhomogeneous and non-uniform in size.

Depth adjustable 3D melanoma model

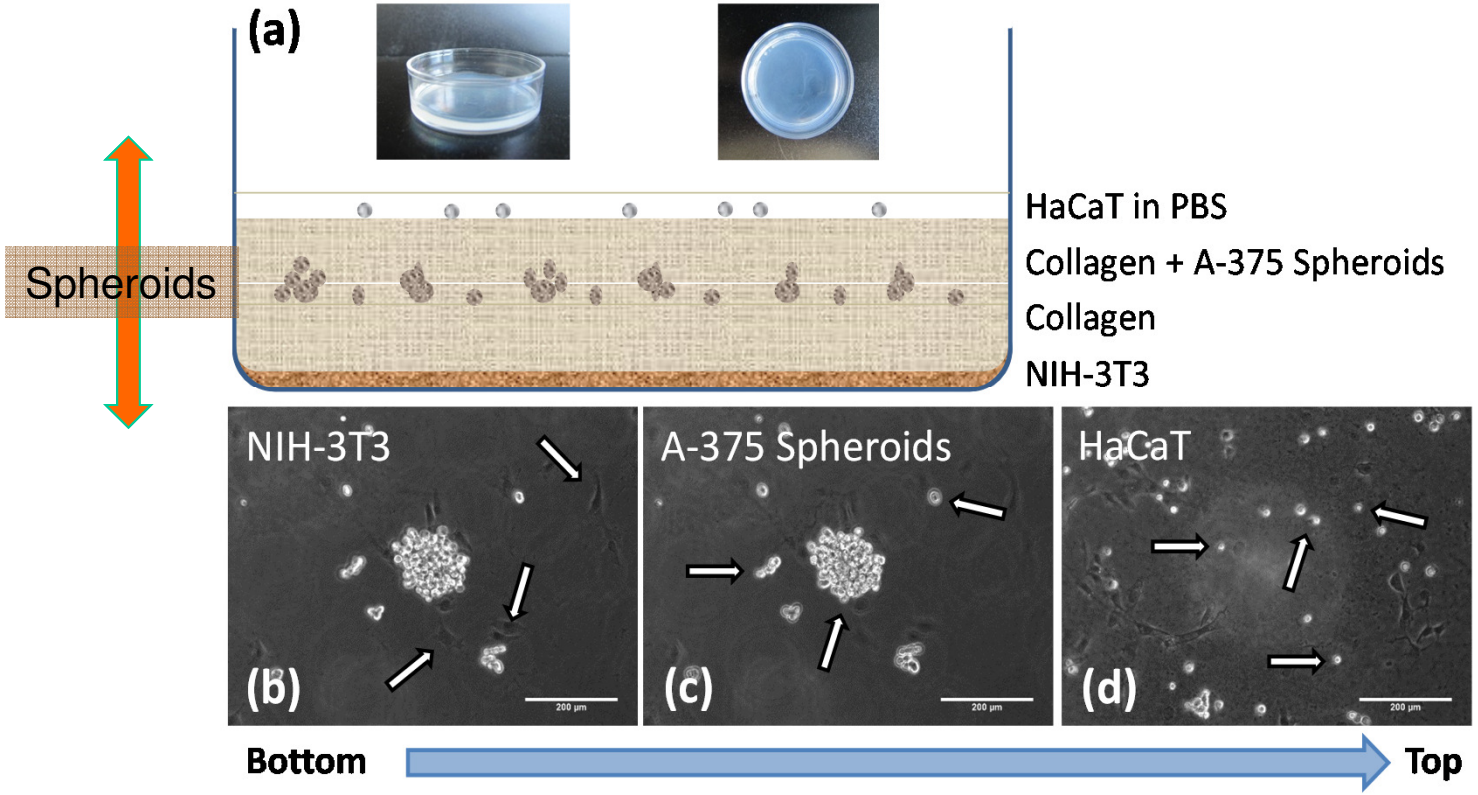

➔ **midIR 3D tissue standards with included tumors can be generate with a precise control of tumor size and position**

Depth adjustable 3D melanoma model

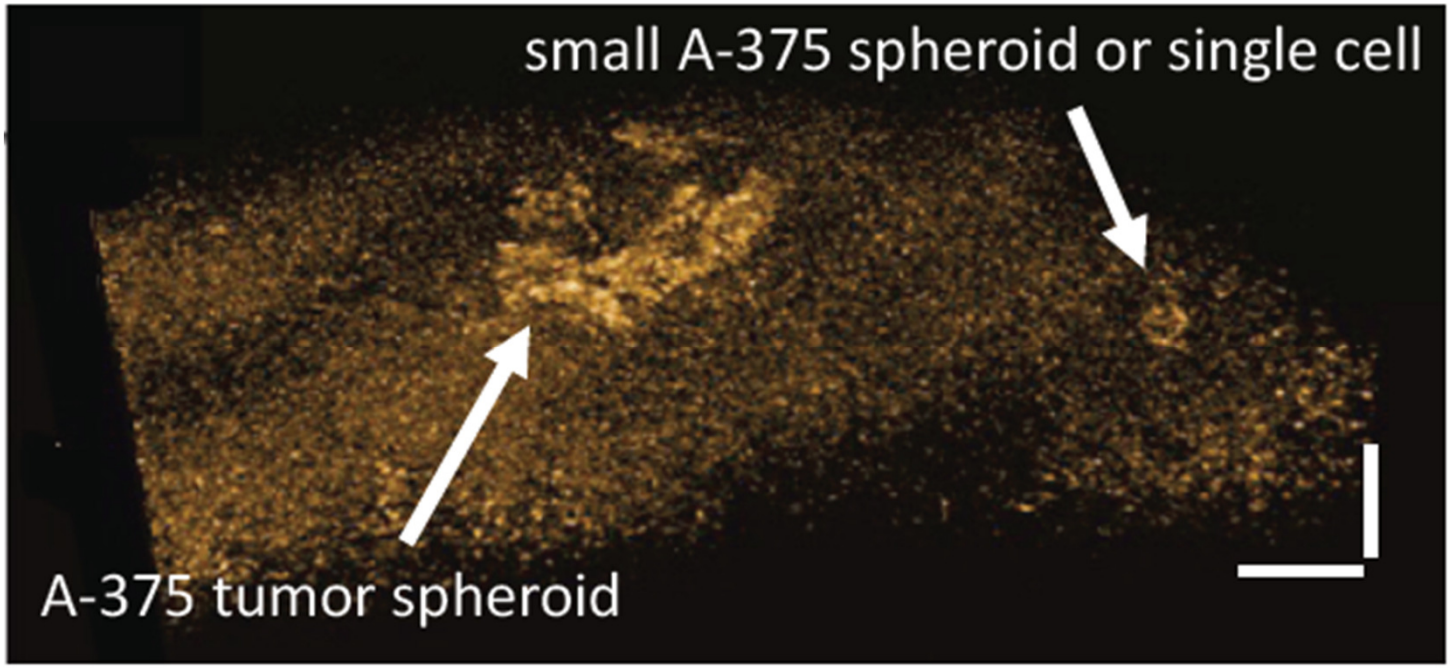

Concept of the simplified 3D tissue standards with different layers and tumor spheroids of different size as well as representative photos of a sample; Documentation of the simplified 3D tissue standards with optical coherence tomography; 3D image of the bottom layer with NIH-3T3 fibroblasts and the collagen layer with included A-375 skin tumor spheroids (indicated with arrows).

Further alternative approaches for tissue samples from HaCats and NIH-3T3

Representative Results (H&E staining)

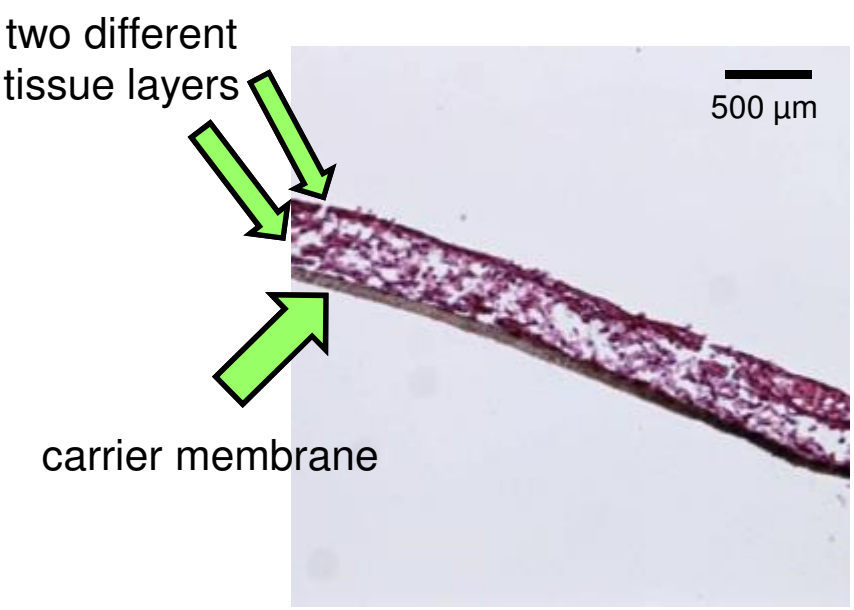

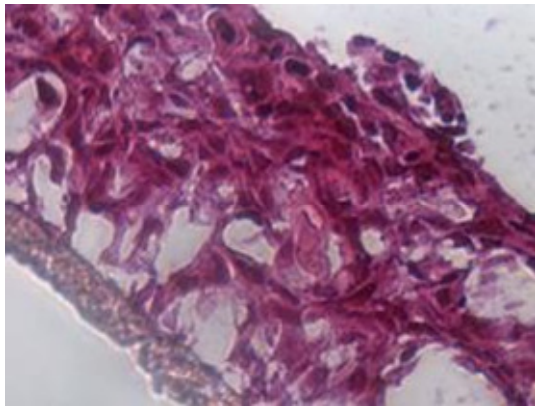

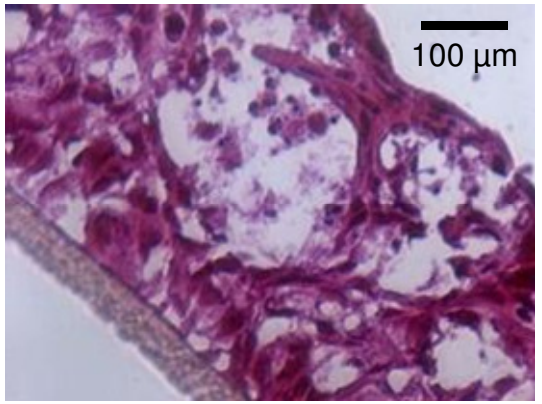

➔ Establishment of further skin substitute standards for midIR spectroscopy

Summary and Conclusions

- Establishment of mid-IR 2D and 3D test samples for human skin and skin cancer with increasing complexity
- Cell types with similar mesenchymal properties can not be separated properly
- Improved algorithms, background subtraction and more measurements for algorithm training may optimize the identification of tumor cell types similar to fibroblasts
- Possibly, the information depth of single cell layers is not sufficient for an accurate image processing
- Complex tissue structures can be accurately differentiated and identified
- Development of 3D melanoma models with tumor cell spheroids and adjustable depth properties
- Newly developed MINERVA cell classification procedures for identification and differentiation demonstrate promising abilities but also critical obstacles for cell type identification specificity
- The obtained spectra showed the potential of mid-IR spectroscopy in the identification of different skin layers and skin structures.

Thank you for your attention!

Skin cancer & cell discrimination using mid-IR spectroscopy

Results from MINERVA WP8

MId- to NEaR infrared spectroscopy
for improVed medical diAgnostics
MINERVA

Westfälische Wilhelms-Universität Münster